

Influence of Charge Fraction on the Phase Behavior of Symmetric Single-Ion Conducting Diblock Copolymers

Bo Zhang, Caini Zheng, Michael B. Sims, Frank S. Bates,* and Timothy P. Lodge*



Cite This: *ACS Macro Lett.* 2021, 10, 1035–1040



Read Online

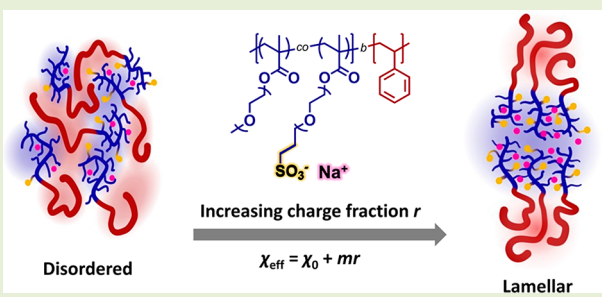
ACCESS |

Metrics & More

Article Recommendations

Supporting Information

ABSTRACT: A series of symmetric poly[(oligo(ethylene glycol) methyl ether methacrylate)-*co*-oligo(ethylene glycol) propyl sodium sulfonate methacrylate]-*block*-polystyrene (PsOEGMA-PS) diblock copolymers were synthesized as a model system to probe the effect of charge fraction on the phase behavior of charged-neutral single-ion conducting diblock copolymers. Small-angle X-ray scattering (SAXS) experiments showed that increasing the charge fraction does not alter the ordered phase morphology (lamellar) but increases the order-disorder transition temperature (T_{ODT}) significantly. Additionally, the effective Flory–Huggins interaction parameter (χ_{eff}) was found to increase linearly with the charge fraction, similar to the case of conventional salt-doped diblock copolymers. This indicates that the effect of counterion solvation, attributed to the significant mismatch between the dielectric constant of each block, provides the dominant effect in tuning the phase behavior of this charged diblock copolymer. We therefore infer that electrostatic cohesion (local charge ordering induced by Coulombic interactions), which is predicted to suppress microphase separation and lead to asymmetric phase diagrams, only plays a minor role in this model system.



In recent years, solid polymer electrolytes (SPEs) have gained significant scientific interest as potential replacements for flammable liquid electrolytes in lithium batteries.^{1–3} A key challenge in designing SPEs with properties competitive to liquid electrolytes is to achieve good ionic conductivity without compromising mechanical integrity. This is difficult to achieve in single-component systems since good ionic conductivity requires high chain mobility while mechanical integrity requires chain rigidity. A well-recognized strategy is to use block copolymers (BCPs) that can self-assemble into periodic nanostructures featuring distinct ion-conducting and mechanically stable phases that can be engineered separately. The most widely studied of such systems is salt-doped poly(ethylene oxide)-*block*-polystyrene (PEO-*b*-PS), in which the PEO domain solvates ions and provides ionic conductivity, while the PS domain provides structural integrity due to its high glass transition temperature (T_g).^{4–10} Nevertheless, these salt-doped systems suffer from limitations such as electrode polarization and modest Li-ion transference number arising from the presence of mobile anions.^{11,12} These issues can be mitigated by developing single-ion conducting polymers (ionomers and polyelectrolytes), where anions are covalently attached to the polymer backbone and thus immobile.^{11,12} Despite an increasing number of reports of single-ion conductors with good conductivity,^{13–19} rational design of single-ion conducting block copolymers remains challenging, due in part to a lack of thorough understanding of the self-assembly of charged diblock copolymers.

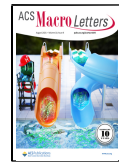
Conventional charge-free diblock copolymers can self-assemble into a host of nanostructures, including lamellae (LAM), cylinders, double gyroid, and spheres.^{20,21} In the classical picture of diblock copolymers, self-assembly behavior is primarily controlled by the block volume fraction f and segregation strength χN , where χ is the Flory–Huggins interaction parameter and N is the degree of polymerization.^{22,23} Self-consistent field theory (SCFT) predicts that an order–disorder transition (ODT) occurs at $\chi N_{ODT} = 10.5$ for symmetric diblock copolymers ($f = 1/2$) in the mean-field limit.²⁴ At finite molecular weights, composition fluctuations stabilize the disordered (DIS) phase in the vicinity of the ODT, thus increasing χN_{ODT} (decreasing T_{ODT}).²⁵

Introduction of charges, either by exogenously doping salts or covalently functionalizing neutral BCPs with charged moieties, significantly alters the phase behavior. For example, experimental studies on doping BCPs, such as poly(methyl methacrylate)-*b*-poly[oligo(ethylene oxide) methacrylate] (PMMA-*b*-POEM),²⁶ polyisoprene-*b*-PEO-*b*-PS,²⁷ PS-*b*-PMMA,²⁸ PS-*b*-PEO,^{5–10} and PS-*b*-poly(2-vinylpyridine),^{29,30} with lithium salts have shown significant increases in χ and

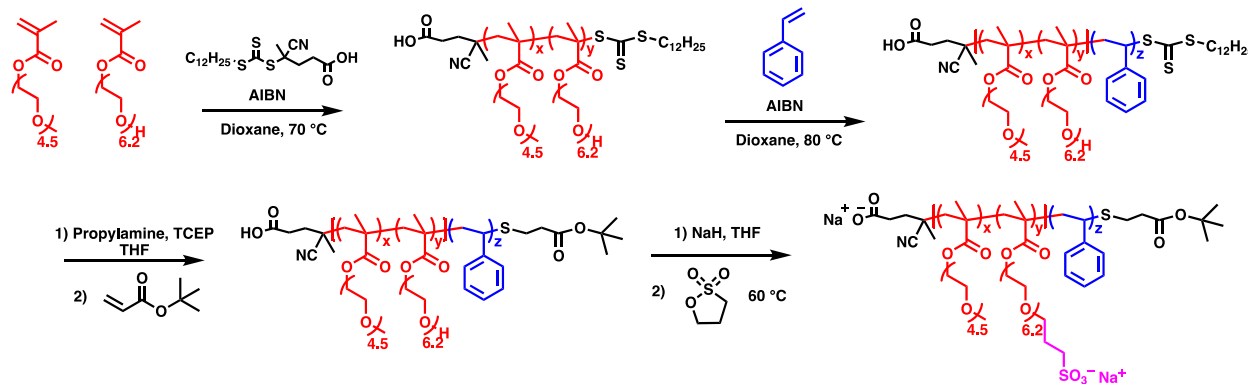
Received: June 11, 2021

Accepted: July 20, 2021

Published: July 23, 2021



Scheme 1. Synthetic Scheme of PsOEGMA-PS



domain spacing, compared to the neat counterparts. In most cases, the effective χ (χ_{eff}) was found to increase linearly with the salt concentration $r = [\text{Li}^+]/[\text{EO}]$, e.g., $\chi_{\text{eff}} = \chi_0 + mr$, where χ_0 pertains to the neat system; m is a system-dependent fitting parameter; and r represents the ratio of lithium cations to ethylene oxide repeat units. Covalently attaching charges to polymer backbones complicates the thermodynamics of self-assembly even further, and depending on the strength of electrostatic interactions, both conventional and unconventional BCP self-assembly can be observed.³¹ For example, morphologies including LAM, double gyroid, and cylinders were identified in symmetric poly(4-styrenesulfonic acid)-*b*-poly(methyl butylene), while only LAM is expected for symmetric neutral BCPs.³² Inverse hexagonally packed cylinders, where the minority-component charged block forms the continuous matrix, have been identified in several systems as well, providing new insight into the structure-conductivity relationships.^{33–35} In contrast to these unconventional self-assembled structures, phase behavior that resembles the self-assembly of neutral BCPs has also been reported.^{36–39}

These intriguing experimental results have motivated extensive theoretical studies to understand the thermodynamics of charged BCPs. Wang and co-workers have incorporated ion dissociation, ion binding, and ion solvation energy into the SCFT to model salt-doped PEO-PS and have successfully captured major experimental observations such as the increase in χ and domain spacing and the dependence of χ on the anion size.^{40–44} Recently, Qin and co-workers have developed a field theory considering solvated ions as “free” ions and predicted distorted phase diagrams for such salt-containing systems.^{45,46} The thermodynamics of charged-neutral block copolyelectrolytes has been investigated by several research groups as well.^{47–52} In particular, Olvera de la Cruz and co-workers have developed a hybrid “liquid state theory + SCFT”, which captures the length scales of both polymer chain conformation and local ion clusters and thus accounts for electrostatic interactions explicitly.^{53–56} Applying this approach to diblock copolyelectrolytes, Sing et al. demonstrated that counterion solvation favors microphase separation captured by $\chi_{\text{eff}} = \chi_0 + mr$ when the charged block has a higher dielectric constant ϵ , consistent with previous studies.^{40–44} In contrast to the relatively straightforward effects of counterion solvation, Coulombic interactions lead to short-range ion clusters involving ions on the polymers as well as counterions. Such electrostatic cohesion results in distorted and “chimney-like” phase diagrams and unconventional morphologies such as inverse hexagonally packed cylinders.⁵⁰

Until now, experimental studies have not addressed the extent to which charge fraction affects χ_{eff} for diblock copolymers with a charged block. In this letter, we report the phase behavior of a series of symmetric poly[(oligo(ethylene glycol) methyl ether methacrylate)-*b*-oligo(ethylene glycol) propyl sodium sulfonate methacrylate]-block-polystyrene (PsOEGMA-PS) diblock copolymers with different charge fractions and molecular weights. Small-angle X-ray scattering (SAXS) experiments demonstrated that χ_{eff} increases linearly with the charge fraction, indicating the dominance of the counterion solvation effect in this model system, which we attribute to the significant difference in the dielectric constant of each block. Interestingly, the ordered phase morphology was not affected by the addition of charged moieties.

The polymers studied in this work were synthesized using reversible addition-fragmentation chain transfer (RAFT) polymerization followed by post-modification to install pendent sulfonate groups, as shown in Scheme 1. The chemical structure of PsOEGMA-PS, with its brush-like EO-containing block, enables the covalent attachment of charged moieties to the polymer chain via the pendent hydroxy functional groups. Additionally, the monomers have reactivity ratios close to 1, enabling systematic tuning of charge fractions from 0 to 1 and nearly uniform charge distributions along polymer chains.⁵⁹ Proton nuclear magnetic resonance (¹H NMR) spectroscopy and size exclusion chromatography (SEC) were used to determine the polymer molecular weight, dispersity, volume fraction, and extent of sulfonation (Table 1). Details about the synthesis and characterization procedures are included in the Supporting Information. SAXS experiments were performed to probe polymer morphologies and identify phase transitions. Representative SAXS profiles are presented in Figure 1, and additional SAXS patterns are included in Figure S5.

PsOEGMA_{0.25}-PS(19) exhibits a disordered (DIS) morphology over the entire experimentally accessible temperature range, indicated by the single broad scattering peak; the lower temperature limit reflects the glass transition temperature of the PS block, $T_{g,PS} = 95$ °C, and the upper limit of 240 °C is set to avoid thermal degradation within the experimental time frame. Ordered morphologies were observed when the charge fraction was increased to 40% (PsOEGMA_{0.4}-PS(19)), as indicated by a sharp scattering peak at temperatures below 180 °C. A lamellar (LAM) morphology was assigned to this sample due to a higher-order diffraction peak at $q/q^* = 3$, where q is the scattering wave vector and q^* is the principal scattering peak. LAM/DIS coexistence at 180 °C is attributed

Table 1. Summary of Polymer Characteristics

name ^a	M_n (kDa) ^b	D ^b	x ^c	r ^d	f_{PsOEGMA} ^e
PsOEGMA _{0.25} -PS(19)	19.4	1.12	0.25	0.048	0.56
PsOEGMA _{0.4} -PS(19)	18.5	1.12	0.40	0.073	0.55
PsOEGMA _{0.7} -PS(22)	21.9	1.17	0.70	0.119	0.51
PsOEGMA _{1.0} -PS(21)	20.6	1.18	1.00	0.159	0.53
PsOEGMA ₀ -PS(23)	23.0	1.13	0	0	0.52
PsOEGMA _{0.15} -PS(23)	22.7	1.17	0.15	0.029	0.47
PsOEGMA _{0.25} -PS(23)	23.3	1.13	0.25	0.048	0.49
PsOEGMA _{0.4} -PS(25)	24.5	1.13	0.40	0.073	0.51
PsOEGMA _{0.7} -PS(26)	25.8	1.15	0.70	0.119	0.53
PsOEGMA ₀ -PS(30)	30.2	1.12	0	0	0.49
PsOEGMA _{0.05} -PS(29)	28.8	1.14	0.05	0.010	0.52
PsOEGMA _{0.1} -PS(31)	31.4	1.14	0.10	0.020	0.51
PsOEGMA _{0.15} -PS(30)	29.5	1.17	0.15	0.029	0.52
PsOEGMA _{0.25} -PS(33)	32.7	1.17	0.25	0.048	0.51
PsOEGMA _{0.4} -PS(34)	33.9	1.19	0.40	0.073	0.55

^aPsOEGMA_x-PS(y) is used to name the polymers, where x is the mole fraction of charged monomers in the PsOEGMA block, and y is the molecular weight in kDa. ^bNumber-average molecular weights (M_n) and dispersities (D), determined by SEC in *N,N*-dimethylformamide (DMF) containing 0.05 M LiBr as the eluent. ^cMole fractions (x) of charged monomers, determined using ¹H NMR spectroscopy and matched quantitatively with the target values. ^dCharge fractions (r) in terms of $[\text{Na}^+]/[\text{EO}]$. ^ePsOEGMA volume fractions, obtained using melt density of PS = 1.05 g/cm³,⁵⁷ and melt densities of PsOEGMA₀ = 1.08 g/cm³ and PsOEGMA_{1.00} = 1.18 g/cm³, which were obtained using a group contribution method.⁵⁸

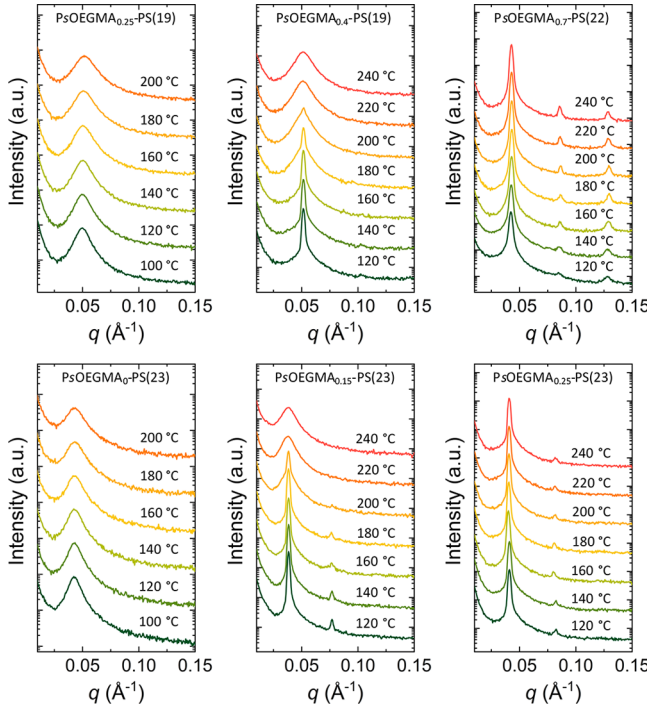


Figure 1. Selected SAXS patterns for polymers with different charge fractions and molecular weights.

to the order–disorder transition (ODT). Results from these two samples suggest that a 15% increase in charge fraction leads to an increase in T_{ODT} of at least 80 °C. Increasing the charge fraction to 70% (PsOEGMA_{0.7}-PS(22)) results in a further significant increase in T_{ODT} (presumably much higher than 240 °C), as the sharp scattering peaks indicating an

ordered LAM morphology persist up to at least 240 °C. At 23 kDa, a LAM morphology appears at 15% charge fraction (PsOEGMA_{0.15}-PS(23)) with an ODT at approximately 180 °C. At 25% charge fraction (PsOEGMA_{0.25}-PS(23)), the LAM morphology persists up to at least 240 °C. Note that the required charge fraction to form an ordered structure decreases from 40% to 15% when the M_n is increased from 19 kDa to 23 kDa. Increasing the M_n to 30 kDa corroborates this result, as indicated by the ODT at 205 °C for 0% charge fraction (PsOEGMA₀-PS(30)). With 5% charge fraction (PsOEGMA_{0.05}-PS(29)) the ODT decreases slightly to 190 °C, which is attributed to the small decrease in M_n . The ODT for the specimen with 10% charge fraction (PsOEGMA_{0.1}-PS(31)) is above 240 °C. Together, these results show that increasing the charge fraction increases T_{ODT} considerably at constant M_n , indicating a strong increase in the effective segregation strength, reflected in χ_{eff} . Increasing M_n while maintaining the charge fraction constant also promotes ordering, consistent with numerous previous results from neutral BCPs.²¹ We have summarized these results in three phase portraits, as shown in Figure 2, where each figure corresponds to a specific molecular weight. Notably, LAM is the only ordered morphology found

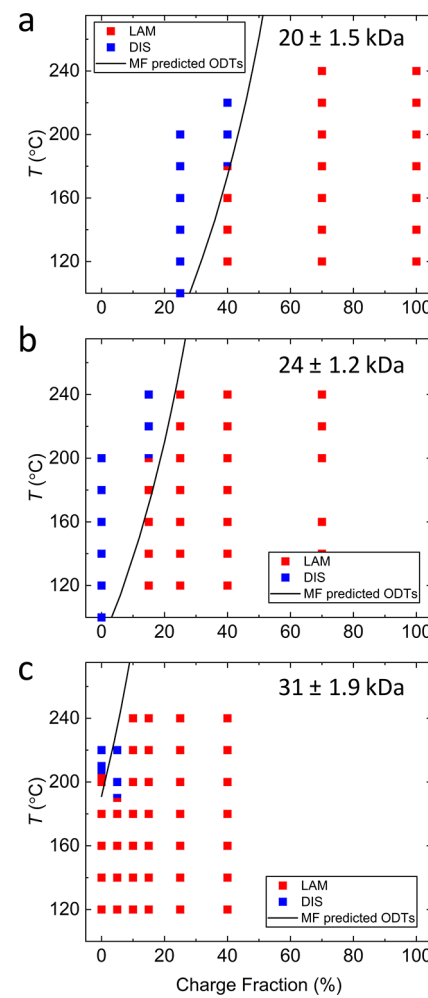


Figure 2. Phase portraits as a function of charge fraction for polymers with average molecular weights of (a) 20 kDa, (b) 24 kDa, and (c) 31 kDa. Red squares are LAM; blue squares are DIS; and black lines are ODT lines predicted using mean-field theory.

in all the specimens, suggesting that no significant change in interfacial curvature occurs upon the addition of charge.

Several equations have been proposed in the literature to model χ_{eff} as a function of added salt concentration.^{7,26} It turns out that the simplest case, $\chi_{\text{eff}} = \chi_0 + mr$, can describe χ_{eff} for the current PsOEGMA-PS system properly. In this equation, χ_0 is the neat χ for neutral diblock copolymers; typically, $\chi_0 = \alpha/T + \beta$ where α , β , and m are system-dependent fitting parameters. Here we assume χ_0 is independent of charge fraction r and degree of polymerization N . To obtain α and β , we prepared a series of symmetric neutral diblock copolymers with different average molecular weights by blending two symmetric samples (23 kDa and 30 kDa). These mixtures show a decrease in T_{ODT} from 205 to 115 °C when M_n is decreased from 30.2 kDa to 25.5 kDa. The SAXS patterns for these mixtures are presented in the Supporting Information (Figure S6). We obtained χ_0 using the mean-field result, $\chi_0 = 10.5/N$ at the ODT,²⁴ and plotted the resulting χ_0 against $1/T_{\text{ODT}}$ to obtain α and β (Figure 3a). Here N is based on a reference volume of 0.1 nm³.

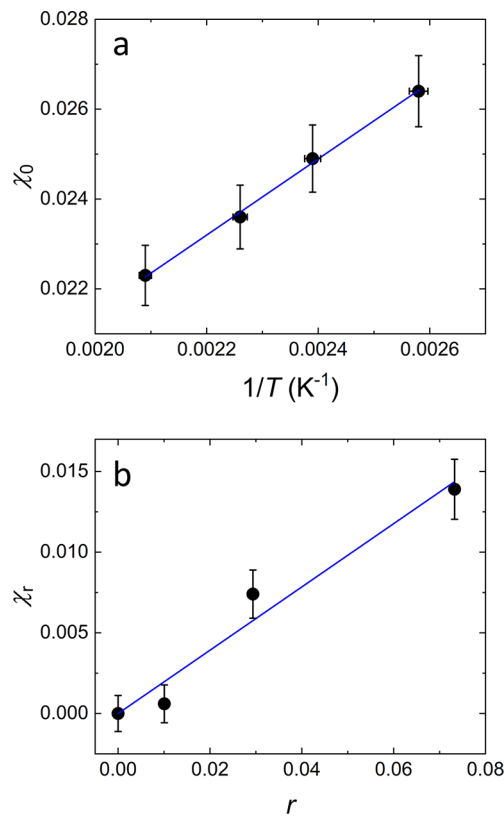


Figure 3. (a) Plot of χ_0 versus $1/T$ to obtain α and β . (b) Plot of χ_r versus r to obtain m .

Interestingly, the obtained χ_0 is only about half of $\chi_{0,\text{PEO-PS}}$ at comparable temperatures: $\chi_{0,\text{POEGMA-PS}} \approx 0.02$ and $\chi_{0,\text{PEO-PS}} \approx 0.05$ at 100 °C.⁴ The difference likely arises from the short-chain branched architecture of POEGMA: possibly the EO units closer to the backbone are less likely to contact S repeat units, which reduces the number of effective contacts between the EO and S repeat units and thus χ_0 , consistent with results from previous studies.^{60,61} With α and β established, mr (i.e., χ_r) at different charge fractions can be derived by subtracting $\alpha/T_{\text{ODT}} + \beta$ from χ_{eff} , which again was obtained using $\chi_{\text{eff}}N = 10.5$ at the ODT.²⁴ A plot of χ_r versus r gives a clear linear relationship (Figure 3b), where the slope yields m . Overall, this

analysis provides the following relationship for the effective Flory–Huggins interaction parameter:

$$\chi_{\text{eff}} = 8.56/T + 0.0044 + 0.196r \quad (1)$$

Since this expression was obtained by fitting two independent sets of ODT information (α and β from neutral polymers and m from charged polymers), it is important to assess whether this expression can properly describe the phase behavior in each phase diagram individually. To do this, we used the mean-field result of $\chi_{\text{eff}}N = 10.5$ at the ODT to calculate χ_{eff} for each M_n . Then we obtained $\alpha/T_{\text{ODT}} + \beta$ from $\chi_{\text{eff}} - mr$ at each charge fraction, which in turn gave T_{ODT} at each charge fraction. The results are shown in Figure 2 as the black lines, which almost quantitatively capture the phase boundaries between LAM and DIS. This reinforces the appropriateness of using $\chi_0 + mr$ to model χ_{eff} . Note that small variations in M_n exist among each set of polymers. The ODT curve in each phase portrait was calculated using M_n of 19 kDa, 24.5 kDa, and 30 kDa, respectively, slightly different from the average M_n in each case (less than 5% difference).

As shown by Sing et al., counterion solvation energy favors microphase separation when the charged block has a higher dielectric constant ϵ .⁵⁰ On the other hand, electrostatic cohesion enhances microphase separation when the volume fraction of the charged block is small (e.g., $f < 0.3$) but suppresses microphase separation when f is increased.⁵⁰ The dielectric constant for neutral POEGMA is $\epsilon_{\text{POEGMA}} \approx 11$, although the actual value is likely higher when the sodium sulfonate group is included;⁶² the dielectric constant for PS is $\epsilon_{\text{PS}} \approx 2.5$. This significant difference in ϵ is expected to shift the phase boundaries toward lower $\chi_{\text{eff}}N$, compared to the neutral case, based solely on counterion solvation. Electrostatic cohesion, on the other hand, should suppress microphase separation since the polymers examined here are compositionally symmetric.⁵⁰ Together these two effects could lead to a complicated expression for χ_{eff} . Since $\chi_{\text{eff}} = \chi_0 + mr$ successfully accounts for the experimental results, we conclude that the effects of counterion solvation overwhelm those of electrostatic neutral POEGMA-PS doped with lithium salts cohesion, thus dominating the change in intermolecular interactions in this model system. We attribute this to the large mismatch between ϵ_{POEGMA} and ϵ_{PS} . Dominance of counterion solvation is further corroborated by persistence of the LAM morphology across all specimens and temperatures, consistent with other results when electrostatic interaction is relatively weak.^{36–39} In order to isolate the effects of electrostatic cohesion, model systems with more closely matched ϵ but non-negligible χ_0 must be designed.⁵⁰ This may be nontrivial because the cohesive energy density is related to ϵ , and the difference in cohesive energy density usually (although not always) determines χ_0 .

Interestingly, the linear dependence of χ_{eff} on charge fraction, characterized by m , is similar to the result obtained from neutral POEGMA-PS doped with lithium salts (e.g., $m \approx 0.3$ for LiCF_3SO_3), although a direct comparison of m values may not be appropriate due to the difference in ion identities and methods used to obtain m .⁶¹ In salt-doped PEO-PS systems, cation identity only plays a minimal role in the phase behavior, while anion solvation dominates χ_{eff} .⁶ This is expected to apply to the case of salt-doped POEGMA-PS as well. In the current system, it is not clear how the type of cation and anion affects χ_{eff} . However, since the anions are chemically bonded to the polymer chains, we anticipate they behave qualitatively differently than the anions in the salt-

doped mixtures. In this case, ion solvation only comes from the mobile cations. Anions still influence χ_{eff} by changing the chemical structure of the monomers, rather than imposing ion solvation energy. The phase behavior of these model polymers with different anions and cations will be addressed in a future publication.

In this work, we report the phase behavior of a series of symmetric charged-neutral single-ion conducting diblock copolymers with different charge fractions and molecular weights. We found that the tethered charges do not alter the ordered LAM morphology but significantly increase T_{ODT} and χ_{eff} . A simple linear correction to the Flory–Huggins interaction parameter, $\chi_{\text{eff}} = \chi_0 + mr$, quantitatively accounts for counterion solvation effects associated with the significant mismatch in the dielectric constant of each block. Additionally, the dependence of χ_{eff} on charge fraction is similar to the case of doping lithium salts into neutral POEGMA-PS. This work provides important insight into the phase behavior of charged-neutral diblock copolyelectrolytes and will inform the design of nanostructured single-ion conducting polymer electrolytes.

■ ASSOCIATED CONTENT

SI Supporting Information

The Supporting Information is available free of charge at <https://pubs.acs.org/doi/10.1021/acsmacrolett.1c00393>.

Synthesis procedures, characterization details, SEC traces, ^1H NMR spectra, and SAXS patterns ([PDF](#))

■ AUTHOR INFORMATION

Corresponding Authors

Timothy P. Lodge – Department of Chemical Engineering and Materials Science and Department of Chemistry, University of Minnesota, Minneapolis, Minnesota 55455, United States; [orcid.org/0000-0001-5916-8834](#); Email: lodge@umn.edu

Frank S. Bates – Department of Chemical Engineering and Materials Science, University of Minnesota, Minneapolis, Minnesota 55455, United States; [orcid.org/0000-0003-3977-1278](#); Email: bates001@umn.edu

Authors

Bo Zhang – Department of Chemical Engineering and Materials Science, University of Minnesota, Minneapolis, Minnesota 55455, United States; [orcid.org/0000-0001-5366-1855](#)

Caini Zheng – Department of Chemistry, University of Minnesota, Minneapolis, Minnesota 55455, United States

Michael B. Sims – Department of Chemical Engineering and Materials Science, University of Minnesota, Minneapolis, Minnesota 55455, United States; [orcid.org/0000-0002-5308-3386](#)

Complete contact information is available at:

<https://pubs.acs.org/10.1021/acsmacrolett.1c00393>

Notes

The authors declare no competing financial interest.

■ ACKNOWLEDGMENTS

This work was supported by the Office of Basic Energy Sciences (BES) of the U.S. Department of Energy (DoE), under Contract No. DE-FOA-0001664. Parts of this work were carried out in the Characterization Facility at the University of

Minnesota, which receives partial support from the NSF through the MRSEC program (DMR-2011401).

■ REFERENCES

- 1) Tarascon, J.-M.; Armand, M. Issues and Challenges Facing Rechargeable Lithium Batteries. *Nature* **2001**, *414*, 359–367.
- 2) Manthiram, A.; Yu, X.; Wang, S. Lithium Battery Chemistries Enabled by Solid-State Electrolytes. *Nat. Rev. Mater.* **2017**, *2*, 1–16.
- 3) Hallinan, D. T.; Balsara, N. P. Polymer Electrolytes. *Annu. Rev. Mater. Res.* **2013**, *43*, 503–525.
- 4) Wanakule, N. S.; Panday, A.; Mullin, S. A.; Gann, E.; Hexemer, A.; Balsara, N. P. Ionic Conductivity of Block Copolymer Electrolytes in the Vicinity of Order-Disorder and Order-Order Transitions. *Macromolecules* **2009**, *42*, 5642–5651.
- 5) Young, W.-S.; Epps, T. H. Salt Doping in PEO-Containing Block Copolymers: Counterion and Concentration Effects. *Macromolecules* **2009**, *42*, 2672–2678.
- 6) Wanakule, N. S.; Virgili, J. M.; Teran, A. A.; Wang, Z.-G.; Balsara, N. P. Thermodynamic Properties of Block Copolymer Electrolytes Containing Imidazolium and Lithium Salts. *Macromolecules* **2010**, *43*, 8282–8289.
- 7) Teran, A. A.; Balsara, N. P. Thermodynamics of Block Copolymers with and without Salt. *J. Phys. Chem. B* **2014**, *118*, 4–17.
- 8) Thelen, J. L.; Teran, A. A.; Wang, X.; Garetz, B. A.; Nakamura, I.; Wang, Z.-G.; Balsara, N. P. Phase Behavior of a Block Copolymer/Salt Mixture through the Order-to-Disorder Transition. *Macromolecules* **2014**, *47*, 2666–2673.
- 9) Loo, W. S.; Galluzzo, M. D.; Li, X.; Maslyn, J. A.; Oh, H. J.; Mongcpa, K. I.; Zhu, C.; Wang, A. A.; Wang, X.; Garetz, B. A.; Balsara, N. P. Phase Behavior of Mixtures of Block Copolymers and a Lithium Salt. *J. Phys. Chem. B* **2018**, *122*, 8065–8074.
- 10) Loo, W. S.; Balsara, N. P. Organizing Thermodynamic Data Obtained from Multicomponent Polymer Electrolytes: Salt-Containing Polymer Blends and Block Copolymers. *J. Polym. Sci., Part B: Polym. Phys.* **2019**, *57*, 1177–1187.
- 11) Zhang, H.; Li, C.; Piszcza, M.; Coya, E.; Rojo, T.; Rodriguez-Martinez, L. M.; Armand, M.; Zhou, Z. Single Lithium-Ion Conducting Solid Polymer Electrolytes: Advances and Perspectives. *Chem. Soc. Rev.* **2017**, *46*, 797–815.
- 12) Zhu, J.; Zhang, Z.; Zhao, S.; Westover, A. S.; Belharouak, I.; Cao, P. F. Single-Ion Conducting Polymer Electrolytes for Solid-State Lithium-Metal Batteries: Design, Performance, and Challenges. *Adv. Energy Mater.* **2021**, *11*, 2003836.
- 13) Inceoglu, S.; Rojas, A. A.; Devaux, D.; Chen, X. C.; Stone, G. M.; Balsara, N. P. Morphology-Conductivity Relationship of Single-Ion-Conducting Block Copolymer Electrolytes for Lithium Batteries. *ACS Macro Lett.* **2014**, *3*, 510–514.
- 14) Rojas, A. A.; Inceoglu, S.; Mackay, N. G.; Thelen, J. L.; Devaux, D.; Stone, G. M.; Balsara, N. P. Effect of Lithium-Ion Concentration on Morphology and Ion Transport in Single-Ion-Conducting Block Copolymer Electrolytes. *Macromolecules* **2015**, *48*, 6589–6595.
- 15) Fan, F.; Wang, Y.; Hong, T.; Heres, M. F.; Saito, T.; Sokolov, A. P. Ion Conduction in Polymerized Ionic Liquids with Different Pendant Groups. *Macromolecules* **2015**, *48*, 4461–4470.
- 16) Choi, U. H.; Lee, M.; Wang, S.; Liu, W.; Winey, K. L.; Gibson, H. W.; Colby, R. H. Ionic Conduction and Dielectric Response of Poly(Imidazolium Acrylate) Ionomers. *Macromolecules* **2012**, *45*, 3974–3985.
- 17) Tudry, G. J.; O'Reilly, M. V.; Dou, S.; King, D. R.; Winey, K. I.; Runt, J.; Colby, R. H. Molecular Mobility and Cation Conduction in Polyether-Ester-Sulfonate Copolymer Ionomers. *Macromolecules* **2012**, *45*, 3962–3973.
- 18) Evans, C. M.; Sanoja, G. E.; Popere, B. C.; Segalman, R. A. Anhydrous Proton Transport in Polymerized Ionic Liquid Block Copolymers: Roles of Block Length, Ionic Content, and Confinement. *Macromolecules* **2016**, *49*, 395–404.
- 19) Evans, C. M.; Bridges, C. R.; Sanoja, G. E.; Bartels, J.; Segalman, R. A. Role of Tethered Ion Placement on Polymerized

Ionic Liquid Structure and Conductivity: Pendant versus Backbone Charge Placement. *ACS Macro Lett.* **2016**, *5*, 925–930.

(20) Bates, F. S.; Fredrickson, G. H. Block Copolymer Thermodynamics: Theory and Experiment. *Annu. Rev. Phys. Chem.* **1990**, *41*, 525–557.

(21) Bates, F. S.; Fredrickson, G. H. Block Copolymers—Designer Soft Materials. *Phys. Today* **1999**, *52*, 32–38.

(22) Flory, P. J. Thermodynamics of High Polymer Solutions. *J. Chem. Phys.* **1942**, *10*, 51–61.

(23) Huggins, M. L. Theory of Solutions of High Polymers. *J. Am. Chem. Soc.* **1942**, *64*, 1712–1719.

(24) Leibler, L. Theory of Microphase Separation in Block Copolymers. *Macromolecules* **1980**, *13*, 1602–1617.

(25) Fredrickson, G. H.; Helfand, E. Fluctuation Effects in the Theory of Microphase Separation in Block Copolymers. *J. Chem. Phys.* **1987**, *87*, 697–705.

(26) Ruzette, A.-V. G.; Soo, P. P.; Sadoway, D. R.; Mayes, A. M. Melt-Formable Block Copolymer Electrolytes for Lithium Rechargeable Batteries. *J. Electrochem. Soc.* **2001**, *148*, A537–A533.

(27) Epps, T. H.; Bailey, T. S.; Waletzko, R.; Bates, F. S. Phase Behavior and Block Sequence Effects in Lithium Perchlorate-Doped Poly(Isoprene-*b*-Styrene-*b*-Ethylene Oxide) and Poly(Styrene-*b*-Isoprene-*b*-Ethylene Oxide) Triblock Copolymers. *Macromolecules* **2003**, *36*, 2873–2881.

(28) Wang, J. Y.; Chen, W.; Russell, T. P. Ion-Complexation-Induced Changes in the Interaction Parameter and the Chain Conformation of PS-*b*-PMMA Copolymers. *Macromolecules* **2008**, *41*, 4904–4907.

(29) Naidu, S.; Ahn, H.; Gong, J.; Kim, B.; Ryu, D. Y. Phase Behavior and Ionic Conductivity of Lithium Perchlorate-Doped Polystyrene-*b*-Poly(2-Vinylpyridine) Copolymer. *Macromolecules* **2011**, *44*, 6085–6093.

(30) Gunkel, I.; Thurn-Albrecht, T. Thermodynamic and Structural Changes in Ion-Containing Symmetric Diblock Copolymers: A Small-Angle X-Ray Scattering Study. *Macromolecules* **2012**, *45*, 283–291.

(31) Wang, X.; Goswami, M.; Kumar, R.; G. Sumpter, B.; Mays, J. Morphologies of Block Copolymers Composed of Charged and Neutral Blocks. *Soft Matter* **2012**, *8*, 3036–3052.

(32) Park, M. J.; Balsara, N. P. Phase Behavior of Symmetric Sulfonated Block Copolymers. *Macromolecules* **2008**, *41*, 3678–3687.

(33) Goswami, M.; Sumpter, B. G.; Huang, T.; Messman, J. M.; Gido, S. P.; Isaacs-Sodeye, A. I.; Mays, J. W. Tunable Morphologies from Charged Block Copolymers. *Soft Matter* **2010**, *6*, 6146–6154.

(34) Russell, S. T.; Raghunathan, R.; Jimenez, A. M.; Zhang, K.; Brucks, S. D.; Iacob, C.; West, A. C.; Gang, O.; Campos, L. M.; Kumar, S. K. Impact of Electrostatic Interactions on the Self-Assembly of Charge-Neutral Block Copolyelectrolytes. *Macromolecules* **2020**, *53*, 548–557.

(35) Zhang, W.; Liu, Y.; Jackson, A. C.; Savage, A. M.; Ertem, S. P.; Tsai, T. H.; Seifert, S.; Beyer, F. L.; Liberatore, M. W.; Herring, A. M.; Coughlin, E. B. Achieving Continuous Anion Transport Domains Using Block Copolymers Containing Phosphonium Cations. *Macromolecules* **2016**, *49*, 4714–4722.

(36) Scalfani, V. F.; Wiesnauer, E. F.; Ekblad, J. R.; Edwards, J. P.; Gin, D. L.; Bailey, T. S. Morphological Phase Behavior of Poly(RTIL)-Containing Diblock Copolymer Melts. *Macromolecules* **2012**, *45*, 4262–4276.

(37) Weber, R. L.; Ye, Y.; Schmitt, A. L.; Banik, S. M.; Elabd, Y. A.; Mahanthappa, M. K. Effect of Nanoscale Morphology on the Conductivity of Polymerized Ionic Liquid Block Copolymers. *Macromolecules* **2011**, *44*, 5727–5735.

(38) Choi, J. H.; Ye, Y.; Elabd, Y. A.; Winey, K. I. Network Structure and Strong Microphase Separation for High Ion Conductivity in Polymerized Ionic Liquid Block Copolymers. *Macromolecules* **2013**, *46*, 5290–5300.

(39) Sudre, G.; Inceoglu, S.; Cotanda, P.; Balsara, N. P. Influence of Bound Ion on the Morphology and Conductivity of Anion-Conducting Block Copolymers. *Macromolecules* **2013**, *46*, 1519–1527.

(40) Wang, Z.-G. Effects of Ion Solvation on the Miscibility of Binary Polymer Blends. *J. Phys. Chem. B* **2008**, *112*, 16205–16213.

(41) Nakamura, I.; Balsara, N. P.; Wang, Z.-G. Thermodynamics of Ion-Containing Polymer Blends and Block Copolymers. *Phys. Rev. Lett.* **2011**, *107*, 1–5.

(42) Nakamura, I.; Wang, Z.-G. Salt-Doped Block Copolymers: Ion Distribution, Domain Spacing and Effective χ Parameter. *Soft Matter* **2012**, *8*, 9356–9367.

(43) Nakamura, I.; Balsara, N. P.; Wang, Z.-G. First-Order Disordered-to-Lamellar Phase Transition in Lithium Salt-Doped Block Copolymers. *ACS Macro Lett.* **2013**, *2*, 478–481.

(44) Nakamura, I.; Wang, Z.-G. Thermodynamics of Salt-Doped Block Copolymers. *ACS Macro Lett.* **2014**, *3*, 708–711.

(45) Hou, K. J.; Qin, J. Solvation and Entropic Regimes in Ion-Containing Block Copolymers. *Macromolecules* **2018**, *51*, 7463–7475.

(46) Hou, K. J.; Loo, W. S.; Balsara, N. P.; Qin, J. Comparing Experimental Phase Behavior of Ion-Doped Block Copolymers with Theoretical Predictions Based on Selective Ion Solvation. *Macromolecules* **2020**, *53*, 3956–3966.

(47) Marko, J. F.; Rabin, Y. Microphase Separation of Charged Diblock Copolymers: Melts and Solutions. *Macromolecules* **1992**, *25*, 1503–1509.

(48) Kumar, R.; Muthukumar, M. Microphase Separation in Polyelectrolytic Diblock Copolymer Melt: Weak Segregation Limit. *J. Chem. Phys.* **2007**, *126*, 214902.

(49) Yang, S.; Vishnyakov, A.; Neimark, A. V. Self-Assembly in Block Polyelectrolytes. *J. Chem. Phys.* **2011**, *134*, 054104.

(50) Sing, C. E.; Zwanikken, J. W.; Olvera de la Cruz, M. Electrostatic Control of Block Copolymer Morphology. *Nat. Mater.* **2014**, *13*, 694–698.

(51) Ma, B.; Olvera de la Cruz, M. A Perspective on the Design of Ion-Containing Polymers for Polymer Electrolyte Applications. *J. Phys. Chem. B* **2021**, *125*, 3015–3022.

(52) Gavrilov, A. A.; Chertovich, A. V.; Potemkin, I. I. Phase Behavior of Melts of Diblock-Copolymers With One Charged Block. *Polymers* **2019**, *11*, 1027.

(53) Sing, C. E.; Zwanikken, J. W.; de la Cruz, M. O. Theory of Melt Polyelectrolyte Blends and Block Copolymers: Phase Behavior, Surface Tension, and Microphase Periodicity. *J. Chem. Phys.* **2015**, *142*, 034902.

(54) Sing, C. E.; Olvera de la Cruz, M. Polyelectrolyte Blends and Nontrivial Behavior in Effective Flory-Huggins Parameters. *ACS Macro Lett.* **2014**, *3*, 698–702.

(55) Pryamitsyn, V. A.; Kwon, H. K.; Zwanikken, J. W.; Olvera de la Cruz, M. Anomalous Phase Behavior of Ionic Polymer Blends and Ionic Copolymers. *Macromolecules* **2017**, *50*, 5194–5207.

(56) Jiménez-Ángeles, F.; Kwon, H. K.; Sadman, K.; Wu, T.; Shull, K. R.; Olvera de la Cruz, M. Self-Assembly of Charge-Containing Copolymers at the Liquid-Liquid Interface. *ACS Cent. Sci.* **2019**, *5*, 688–699.

(57) Mark, J. E. *Physical Properties of Polymers Handbook*; Springer, 2007.

(58) Van Krevelen, D. W.; Hoflyzer, P. J. Prediction of Polymer Densities. *J. Appl. Polym. Sci.* **1969**, *13*, 871–881.

(59) Shim, J.; Bates, F. S.; Lodge, T. P. Superlattice by Charged Block Copolymer Self-Assembly. *Nat. Commun.* **2019**, *10*, 1–7.

(60) Ishizone, T.; Han, S.; Hagiwara, M.; Yokoyama, H. Synthesis and Surface Characterization of Well-Defined Amphiphilic Block Copolymers Containing Poly[Oligo(Ethylene Glycol) Methacrylate] Segments. *Macromolecules* **2006**, *39*, 962–970.

(61) Gartner, T. E.; Morris, M. A.; Shelton, C. K.; Dura, J. A.; Epps, T. H. Quantifying Lithium Salt and Polymer Density Distributions in Nanostructured Ion-Conducting Block Polymers. *Macromolecules* **2018**, *51*, 1917–1926.

(62) Bartels, J.; Wang, J.-H. H.; Chen, Q.; Runt, J.; Colby, R. H. Segmental Dynamics of Ethylene Oxide-Containing Polymers with Diverse Backbone Chemistries. *Macromolecules* **2016**, *49*, 1903–1910.